Validation of Finite Element Crash Test Dummy Models for the Prediction of Orion Crew Member Injuries during a Simulated Vehicle Landing

Ala (Al) Tabiei
Mason, Ohio

Charles Lawrence
NASA Glenn Research Center
Cleveland, OH

Edwin L. Fasanella
NASA Langley Research Center
Hampton, VA

Abstract

A series of dummy response during a simulated Crew Exploration Vehicle (CEV) module landing is conducted at the Wright-Patterson Air Force Base (WPAFB). These tests consisted of several crew configurations with, and without astronaut suits. Finite element models of the tests are developed and presented herein. The finite element models are validated using the experimental data. Several outputs from the dummy are collected and presented here in. These outputs are compared with the outputs of the finite element model. Occupant crash data such as forces, moments and accelerations are collected from simulations and compared to the presented injury criteria to assess Occupant Survivability and Human Injury. Some of the injury criteria published in the literature are summarized herein for sake of completeness. These injury criteria are used to determine potential injury during such impact event.

Introduction

During the landing of the Orion crew vehicle on hard surfaces, significant impulse loads could be transmitted to the astronauts through the vehicle-occupant interfaces such as the floor and seat. If these loads are not attenuated to survivable levels, they could lead severe injuries or fatality of the occupants. Simple seat structures are not sufficient to protect the occupant against hard landing, and thus further protective techniques need to be investigated.

Tabiei et al [1] has presented several concepts for pulse mitigation during a high acceleration event. One such concept is an Energy Absorbing Seat Mechanism (EASM) that cushions the occupant against shock pulses by absorbing kinetic energy of the landing and attenuating acceleration pulses transmitted to the occupant to survivable levels.

Concepts that are used in the crashworthiness analysis of aircraft seats could be quite similar to those used in crew protection during the Orion landing. In 1988, Fox [2] performed a feasibility study for an OH-58 helicopter energy attenuating crew seat. Energy attenuating concepts included a pivoting seat pan, a guided bucket, and a tension seat. In 1989, Simula Inc. prepared an Aircraft Crash Survival Design Guide [3] for the Aviation Applied Technology Directorate. The guide outlined various injury criteria, and energy absorbing devices among other such related topics. In 1990, Gowdy [4] designed a crashworthy seat for commuter aircraft using a wire bending energy absorber design. This design was sub-optimal but provided satisfactory results for vertical decelerations between 15-32 Gs. In 1993, Laananen [5] performed a crashworthiness analysis of commuter aircraft seats during full scale impact using SOM-LA (Seat Occupant Model – Light Aircraft). He concluded that those current designs did not meet the then standards for occupant safety, and that vertical direction energy absorbing devices needed to be implemented. In 1994, Haley Jr. [6] evaluated a retrofit OH-58 pilot's seat to study its effectiveness in preventing back injury. In 1996, Alem et al. [7] evaluated an energy absorbing truck seat to evaluate its effectiveness in protection against landmine blasts. In 1998, the Night Vision and Electronic Sensors Directorate published a report on Tactical Wheeled Vehicles and Crew Survivability in Landmine Explosions [8]. The report provides a wealth of information about this topic. In 2002, Kellas [9] designed an energy absorbing seat for an agricultural aircraft using the axial crushing of aluminum tubes as the primary energy absorber. Keeman [10] has briefly summarized the approach adopted during the design of vehicle crashworthy structures that utilize joints and thin walled beams.

The present study focuses on the development of finite element occupant models and finite element analysis of simulated landing events during the Orion landing. The simulations are conducted using the large scale simulation code LSDYNA [26]. The human occupant is simulated by a numerical 50^{th} percentile HYBRID III dummy. Data such as head, chest, and torso acceleration, and dummy-structure contact forces are collected during the simulation and analyzed for injury assessment

In order to determine the effectiveness of the finite element models a validation is performed using test data. A set of experiments are conducted at the Wright-Patterson Air Force Base in Dayton Ohio. These tests are used to validate the finite element crash test dummy models. Occupant crash data such as forces, moments and accelerations are collected from simulations and then compared to these injury criteria to assess Occupant Survivability and Human Injury.

1. Review of Human Injury Tolerance Criteria

In order to determine the effectiveness of a design that protects occupants against injury caused by crash and hard landing injury criteria need to be defined. Occupant crash data such as forces, moments and accelerations are collected from simulations and then compared to these injury criteria to assess Occupant Survivability and Human Injury. Some of the injury criteria published in the literature are summarized herein for sake of completeness [1, 11].

1.1 Generalized Human Tolerance Limits to Acceleration

Table 1 displays the human tolerance limits for typical crash pulses along three mutually orthogonal axes, for a well restrained young male [12]. These values provide a general outline of the safe acceleration limit for a human during a typical crash. However, the time duration of the applied acceleration pulse has not been specified. Higher acceleration pulses can be sustained for shorter durations compare to lower acceleration pulses for longer durations, thus the time duration in question is important.

1.2 Injury Scaling

Injury scaling is a technique for assigning a numerical assessment or severity score to traumatic injuries in order to quantify the severity of a particular injury. The most extensively used injury scale is the Abbreviated Injury Scale (AIS) developed by the American Association for Automotive Medicine and originally published in 1971. The AIS assigns an injury severity of "one" to "six" to each injury according to the severity of each separate anatomical injury. Table 2 provides the AIS designations and gives examples of injuries for the head and spine regions of the body. The primary limitation of the AIS is that it looks at each injury in isolation and does not provide an indication of outcome for the individual as a whole. Consequently, the Injury Severity Score (ISS) was developed in 1974 to predict probability of survival. The ISS is a numerical scale that is derived by summing the squares of the three regions of the body with the highest AIS values. This gives a score ranging from 1 to 75. The maximal value of 75 results from three AIS 5 injuries, or one or more AIS 6 injuries. Probabilities of death have been assigned to each possible score.

1.3 Dynamic Response Index (DRI)

The DRI is representative of the maximum dynamic compression of the vertebral column and is calculated by describing the human body in terms of an analogous, lumped-mass parameter, mechanical model consisting of a mass, spring and damper [27]. The DRI model assesses the response of the human body to transient acceleration-time profiles. DRI has been effective in predicting spinal injury potential for + Gz acceleration environments in ejection seats. DRI is acceptable for evaluation of crash resistant seat performance relative to spinal injury, if used in conjunction with other injury criteria including Eiband and Lumbar Load thresholds [27, 12]. Acceleration limits for the DRI are provided in Table 3.

1.4 Lumbar Load Criterion

The maximum compressive load shall not exceed 1500 pounds (6672 N) measured between the pelvis and lumbar spine of a 50th-percentile test dummy for a crash pulse in which the predominant impact vector is parallel to the vertical axis of the spinal column. Also, the compressive load must not exceed 3800 N in a 30 ms interval. This is one of the most widely used criterions in vertical crash and impact testing. If the spinal cord is severely compressed or severed, it can lead to either instant paralysis or fatality [2, 9, 11-14].

1.5 Head Injury Criterion (HIC)

HIC was proposed by the National Highway Traffic Safety Administration (NHTSA) in 1972 and is an alternative interpretation to the Wayne State Tolerance Curve (WSTC [12, 13]. It is used to assess forehead impact against unyielding surfaces. Basically, the acceleration-time response is experimentally measured and the data is related to skull fractures. Gadd [15] had suggested a weighted-impulse criterion (GADD Severity Index, GSI) as an evaluator of injury potential defined as:

$$SI = \int_t a^n dt \qquad \text{-- (1)}$$

where

SI = GADD Severity Indiex
a = acceleration as a function of time
n = weighting factor greater than 1
t = time

Gadd plotted the WSTC data using a log scale and an approximate straight line function was developed for the weighted impulse criterion that eventually became known as GSI.

The Head Injury Criteria is given by:

$$HIC = (t_2 - t_1)\left[\int_{t_2}^{t_1} a(t)dt\right]^{2.5} \qquad \text{-- (2)}$$

where

a(t) = acceleration as a function of time of the head center of gravity
t_1,t_2 = time limits of integration that maximize HIC

FMVSS 208 (Federal Motor Vehicle Safety and Standards) originally set a maximum value of 1000 for the HIC and specified a time interval not exceeding 36 milliseconds. HIC equal to 1000 represents a 16% probability of a life threatening brain injury. HIC suggests that a higher acceleration for a shorter period is less injurious than a lower level of acceleration for a higher period of time. As of 2000, the NHTSA final rule specified the maximum time limit for calculating the HIC as 15 milliseconds [4, 8, 14-20]. Table 4 shows the HIC for various dummy sizes [12, 14].

TABLE 1: HUMAN TOLERANCE LIMITS TO ACCELERATION

Direction of Accelerative Force	Occupant's Inertial Response	Tolerance Level
Headward (+Gz)	Eyeballs Down	25 G
Tailward (-Gz)	Eyeballs Up	15 G
Lateral Right (+Gy)	Eyeballs Left	20 G
Lateral Left (-Gy)	Eyeballs Right	20 G
Back to Chest (+Gx)	Eyeballs-in	45 G
Chest to Back (-Gx)	Eyeballs-out	45 G

TABLE 2: ABBREVIATED INJURY SCALE (AIS) AND SAMPLE INJURY TYPES FOR TWO BODY REGIONS [12]

AIS	Severity	Head	Spine
0	None	-	-
1	Minor	Headache or Dizziness	Acute Strain (no fracture or dislocation)
2	Moderate	Unconsciousness less than 1 hr., Linear fracture	Minor fracture without any cord involvement
3	Serious	Unconscious, 1-6 hrs., Depressed fracture	Ruptured disc with nerve root damage
4	Severe	Unconscious, 6-24 hrs., Open fracture	Incomplete cervical cord syndrome
5	Critical	Unconscious more than 24 hr, Large hematoma , (100cc)	C4 or below cervical complete cord syndrome
6	Maximum Injury (virtually non-survivable)	Crush of Skull	C3 or above complete cord syndrome

TABLE 3: Dynamic Response Limits from Brinkley and Moser [27]

DR level	**X (eyeballs out, in)**		**Y (eyeballs right, left)**		**Z (eyeballs up, down)**	
	$DR_x < 0$	$DR_x > 0$	$DR_y < 0$	$DR_y > 0$	$DR_z < 0$	$DR_z > 0$
Low (same as NASA spec)	-28	35	-14	14	-13.4	15.2
Moderate	-35	40	-17	17	-16.5	18
High Risk	-46	46	-22	22	-20.4	22.4

TABLE 4: HIC FOR VARIOUS DUMMY SIZES [14]

Dummy Type	Large size Male	Mid size Male	Small size Female	6 year old child	3 year old child	1 year old infant
HIC_{15} Limit	700	700	700	700	570	390

1.6 Head Impact Power (HIP)

A recent report [11] included the proposal of a new HIC entitled Head Impact Power (HIP). This criteria considers not only kinematics of the head (rigid body motion of the skull) but also the change in kinetic energy of the skull which may result in deformation of and injury to the non-rigid brain matter. The Head Impact Power (HIP) is based on the general rate of change of the translational and rotational kinetic energy. The HIP is an extension of previously suggested "Viscous Criterion" first proposed by Lau and Viano in 1986, which states that a certain level or probability of injury will occur to a viscous organ if the product of its compression 'C' and the rate of compression 'V' exceeds some limiting value [11].

1.7 Injury Assessment Reference Values (IARS)

This rule adopts new requirements for specifications, instrumentation, test procedures and calibration for the Hybrid III test dummy [10]. The regulation's preamble has a detailed discussion of the injury mechanisms and the relevant automotive mishap data for each of the injury criteria associated with the Hybrid III ATD. Military test plans should implement these criteria.

1.8 Neck Injury Criterion (NIC)

The NIC considers relative acceleration between the C1 and T1 vertebra and is given by [21]:

$$NIC(t) = 0.2xa_{rel}(t) + [V_{rel}(t)]^2 \quad \text{-- (3)}$$

where

$$a_{rel}(t) = a_x^{T1}(t) - a_x^{Head}(t)$$
$$v_{rel}(t) = \int a_x^{T1}(t) - \int a_x^{Head}(t) \quad \text{-- (4)}$$

NIC must not exceed 15 m^2/s^2 [22]. Another criteria NIC_{50} refers to NIC at 50mm of C1-T1 (cervical-thoracic) retraction. Newly proposed N_{ij} criteria by NHTSA combines effects of forces and moments measured at occipital condyle and is a better predictor of cranio-cervical injuries. N_{ij} takes into account N_{TE} (tension-extension), N_{TF} (tension-flexion), N_{CE} (compression-extension), N_{CF} (compression-flexion). FMVSS specification No.208 requires that none of the four N_{ij} values exceed 1.4 at any point. The generalized NIC is given by [23]:

$$N_{ij} = \left(F_Z / F_{ZC}\right) + \left(M_Y / M_{YC}\right) \quad \text{-- (5)}$$

where F_z = Upper Neck Axial Force (N),
M_y = Moment about Occipital Condyle
F_{zn} = Axial Force Critical Value (N), and
M_{yn} = Moment Critical Value (N-m).

In FMVSS 208 (2000) final rule a neck injury criterion, designated *Nij*, is used. This criterion is based on the belief that the occipital condoyle-head junction can be approximated by a prismatic bar and that the failure for the neck is related to the stress in the ligament tissue spanning the area between the neck and the head. *Nij* must not exceed 1.0 [15, 20, 22, 24]. Table 4 displays the critical values for various dummies used in the calculation of N_{ij} [12].

1.9 Chest Criteria

Peak resultant acceleration will not exceed 60 G's for more than 3 milliseconds (Mertz, 1971) as measured by a Tri-axial accelerometer in upper thorax. Also, the chest compression will be less than 3 inches for the Hybrid III dummy as measured by a chest potentiometer behind the sternum [12, 14].

1.10 Viscous Criterion

Viscous Criterion (V*C) – defined as the chest compression velocity (derived by differentiating the measured chest compression) multiplied by the chest compression and divided by the chest depth. This criterion has been mentioned for the sake of completeness of information; however it is not widely used [11].

1.11 Femur Force Criterion

This criterion states that the compressive force transmitted axially through each upper leg should not exceed a certain value. Impulse loads that exceed this limit can cause complete fracture of the femoral bone as well as sever major arteries that can cause excessive bleeding. Different references state different values for the maximum allowable compressive axial force. Horst et al. [12] uses a maximum of 8000 N for the Tibia Compression Force Criterion. Wayne State University [14] states a maximum allowable value of 10,000 N. The Department of Army [11] states the axial compression force shall not exceed 7562 N in a 10 ms interval and 9074 N at any instant.

In numerical dummies, discrete spring elements of known stiffness are included within the leg model, from which the femur axial compressive force is easily extracted. In actual dummies, load cells are placed on the dummy's leg, which are calibrated to provide the compressive force at the femur.

1.12 Thoracic Trauma Index (TTI)

The Thoracic Trauma Index is given by:

$$TTI(d) = 1/2\,(G_R + G_{LS}) \quad \text{-- (6)}$$

G_R is the greater of the peak accelerations of either the upper or lower rib, expressed in G's. G_{LS} is the lower spine peak acceleration, expressed in G's. The pelvic acceleration must not exceed 130 G's [11].

1.13 Combined Thoracic Index (CTI)

In here the chest defection and the chest acceleration are considered. For a 50th percentile male dummy the chest acceleration should not exceed 60 g's for a 3 ms pulse. The chest deflection should not exceed 63 mm.

Finite Element Dummy Model

The Hybrid III finite element dummy used in this work is developed and validated by Livermore Software Technology Corporation (LSTC). A full set of LSTC Hybrid III finite element dummies are modeled in LSDYNA format. These finite element dummies are then setup according to the ASE calibration procedures for the physical Hybrid III dummies. The dummy finite element model used herein is modeled using rigid and deformable parts. This dummy is validated by LSTC using standard impact tests in four different locations and positions as shown in Figures (1-5). These tests consist of head impact (Figure 1), neck flexion and extension (Figures 3 and 4), chest impact (Figure 2), and knee impact (Figure 5). These tests are selected as this dummy model is validated for crash scenarios observed in car crashes. This dummy however, is not validated for all possible impact scenarios with different orientations. The Hybrid III finite element dummy model by LSTC is free of charge which makes it a good starting point for obtaining initial results for any possible impact situation involving occupant protection.

The dummy model is imported into the preprocessor LSPREPORT to orient the dummy into the desired position. The position of the Hybrid III dummy must match the position of the physical dummy in the test setup. This is achieved by several operations of what is called the "H" point translation and rotation. Limb operations are also available for the proper positions of the hand and legs. The neck, however, is in a standard position that can not be altered. In the new dummy models that are being developed by LSTC, the neck can also be rotated to better match the test set up however this model is not yet completely validated. Since the validated FE neck model cannot be arbitrarily positioned, it is necessary to position the neck in the test dummy to match the FE model for the model to be entirely consistent with the test.

Seat belts are also modeled using the preprocessor LSPREPORT. The Hybrid III finite element is imported into the preprocessor then "segments sets" are defined on the dummy where

the seat belts are to be positioned. Once these sets are defined the seat belt is positioned on the set. The belts are then tensioned to make the belts fit to the contour of the various parts of the dummy where the seat belts contact the dummy. The belts can be modeled with seat belt element (beam like elements) or by shell elements.. The shell model however, is the most appropriate model to capture the seat belt dummy interaction. The pretension in the seat belt is modeled by defining a local coordinate system on the belt ends. A load is then defined in this coordinate system and with a magnitude equal to the preload applied in the test setup. The load however, must be ramped to the full magnitude. Applying the tension to its full magnitude at time zero can lead to unrealistic oscillations in the system response and inaccurate simulation results.

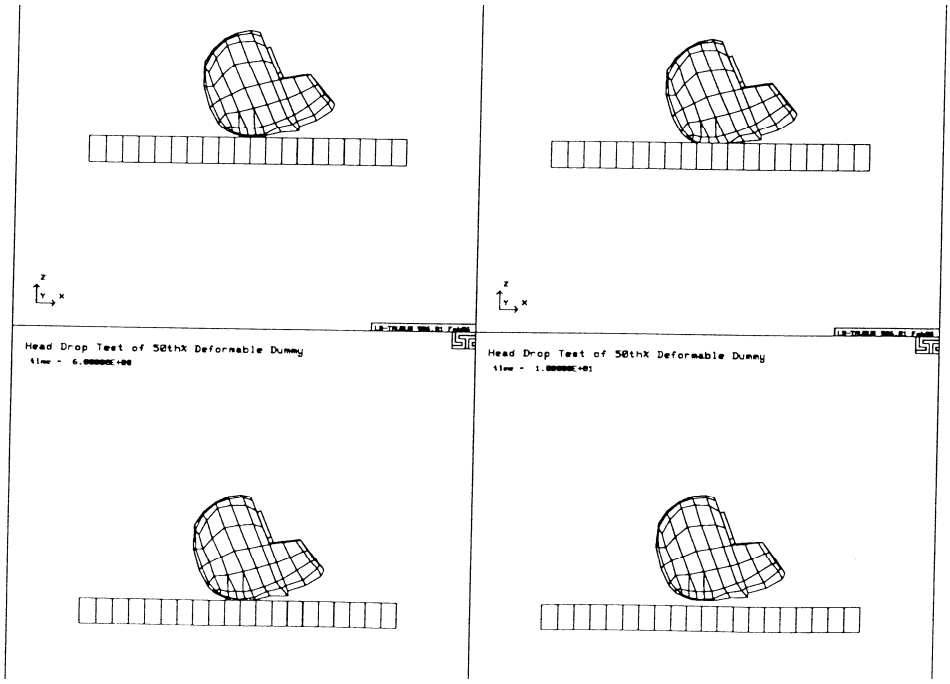

Figure 1. Head model used for test calibration

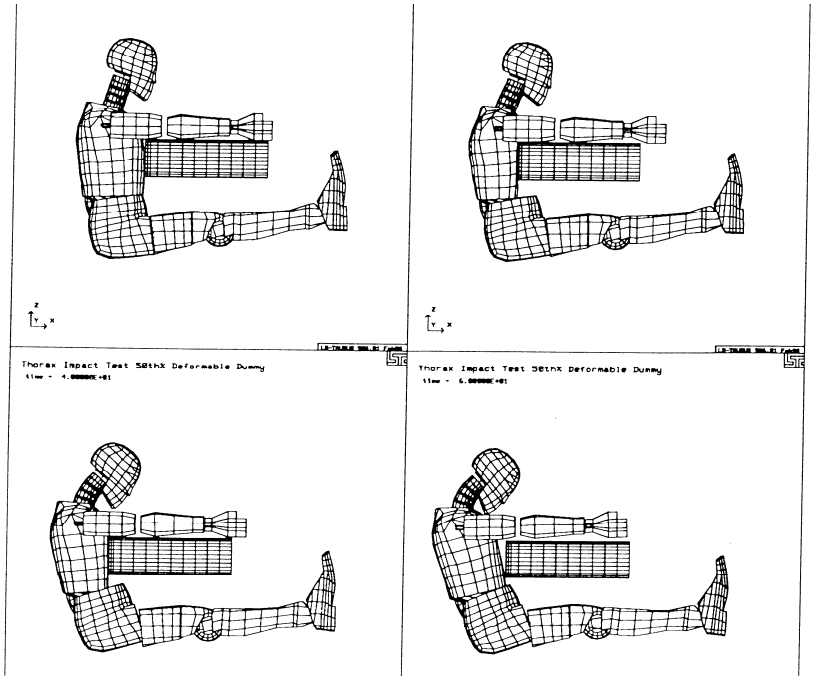

Figure 2. Chest impact calibration

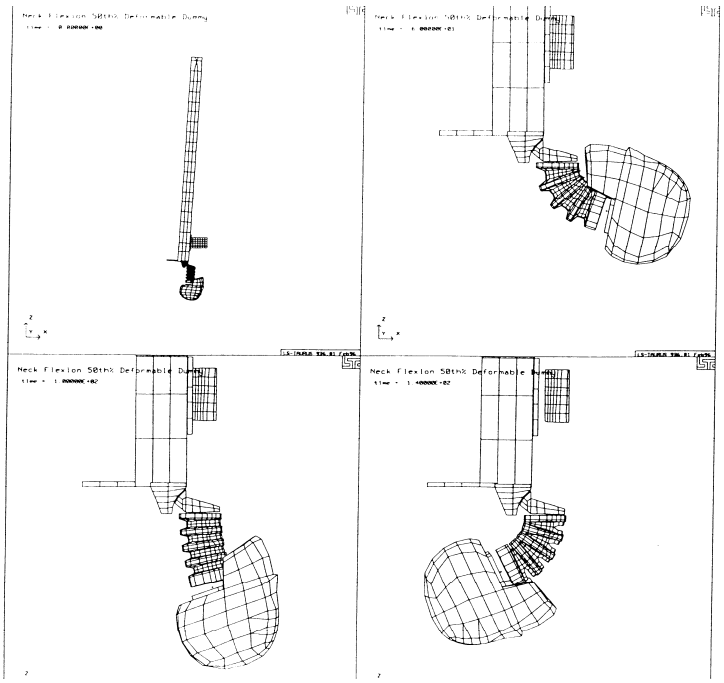

Figure 3. Flexion neck calibration test

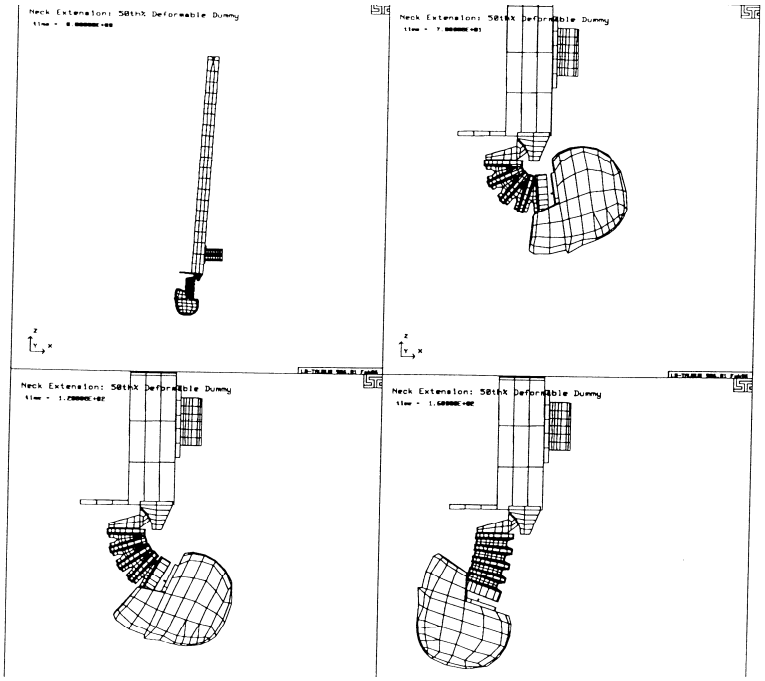

Figure 4. Extension neck calibration test

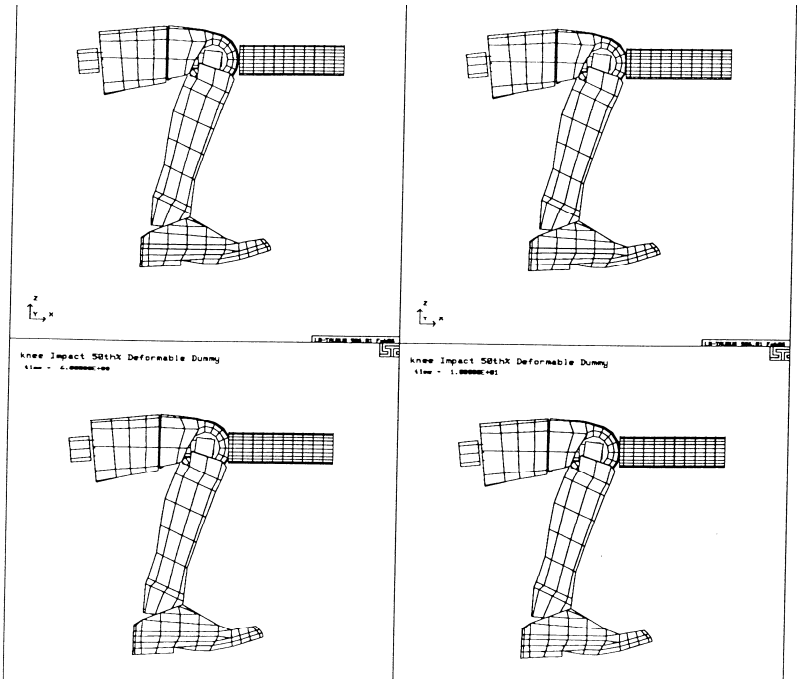

Figure 5. Knee impact calibration test

Hybrid III Dummy Tests

Several sets of experiments are conducted at Wright-Patterson Air Force Base (WPAFB) in Dayton, Ohio. These tests consist of a belted Hybrid III dummy in several configurations and various pulses (see Figures 6-7). In addition, the Hybrid III dummy is clothed in a proposed astronaut suit and tested in several configurations as shown in Figure 8. In the present report only two sets of tests are considered for validation and data extraction. The two tests are the 10 g's pulse in the +x-direction as shown in Figure 6 and the 20 g's pulse in the +z-direction as shown in Figure 7.

The Hybrid III dummy finite element model is positioned similar to the test setup as closely as possible, as shown in Figure 9. However, as previously mentioned, due to the limitation of the Hybrid III finite element neck model the neck in the Hybrid III FE dummy model is pre-set to a fixed location that is typically used in the automotive industry for frontal impact tests. Consequently, the neck position is off by a few degrees with respect to the actual test setup. This difference in neck positioning effects the forces and moments in the neck and the timing of the head impact with the pad located behind the head. The effect is not only in the magnitude of these forces and moments, but also in the phase. The impact between the head and the pads occur at an earlier time because of the placement of these pads between the seat and head. Since the WPAFB testing was performed before the limitation in the FE neck model was identified there was no way to rectify the discrepancy in the neck positions. However, for future testing it would be beneficial to include any constraints in the FE dummy model as part of the test plan. In addition to the neck position, the pad placed between the dummy head and the seat creates uncertainties since the pad thickness and material characteristics unknown. In the simulation assumptions are made to best fit the head data reported from the experimental testing.

The feet and hand positions, as shown from Figure 9, are different between the finite element model and the test set up. However, it was concluded from several simulations that these limbs have very little effect on the kinematics of the chest, head and pelvis. In addition, the limbs did not have any significant effects on the forces and moments collected at various locations/parts of the dummy in the simulation.

The simulation is conducted as close as possible to the test setup. However, due to the neck/head dummy position, a miss-match between the dummy in the test and the dummy in the simulation, some discrepancy in the predictions are possible and expected.

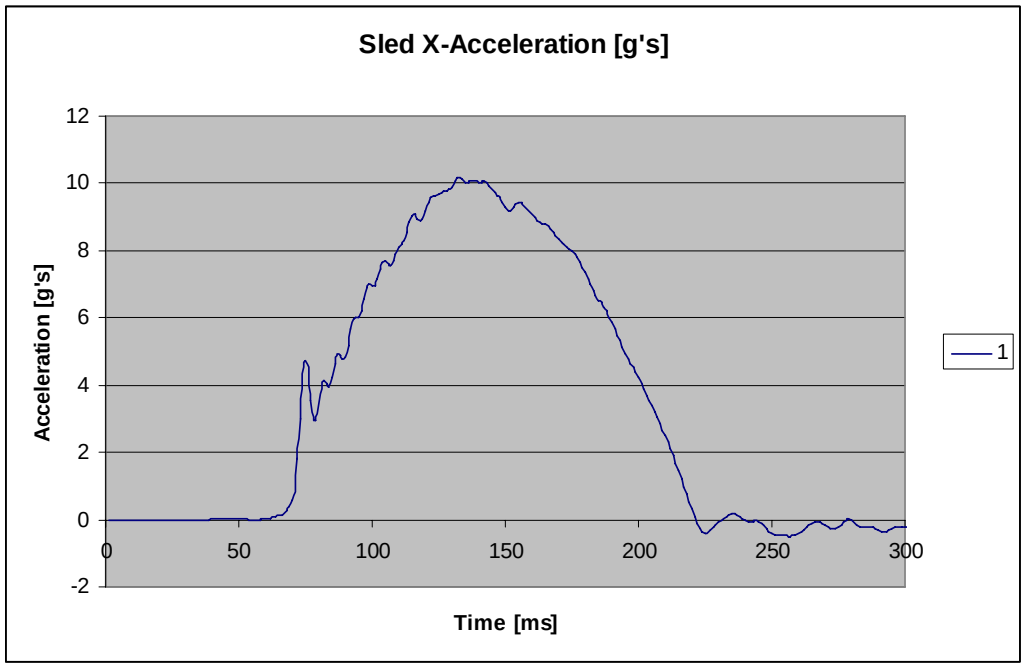

Figure 6. Dummy position in the x-direction with 10 g's impulse

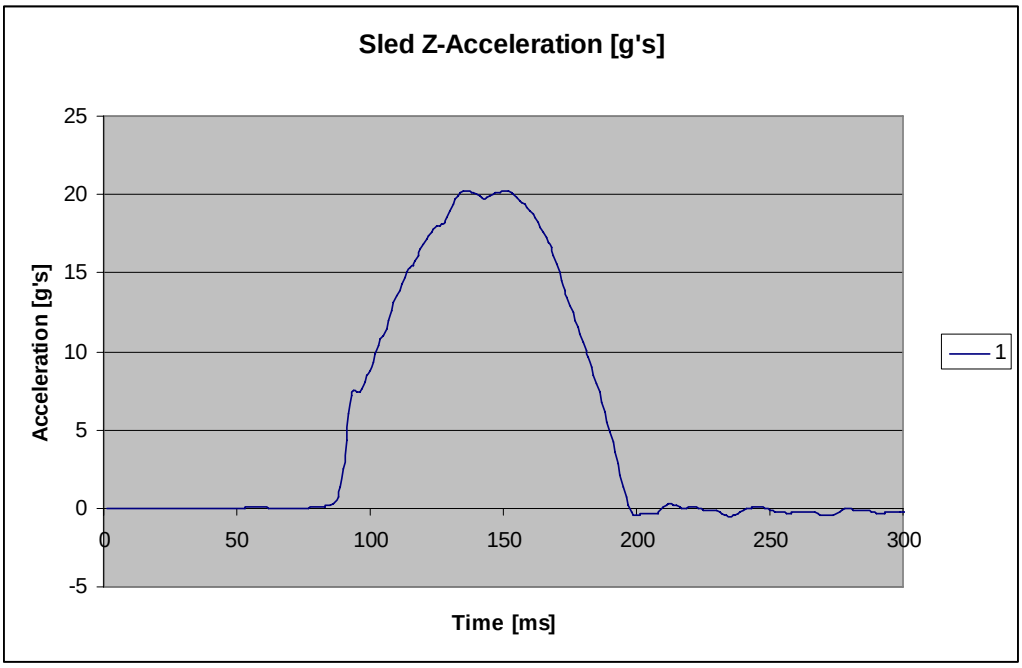

Figure 7. Dummy position in the z-direction with 20 g's impulse

Figure 8. Hybrid III with a proposed astronaut suit

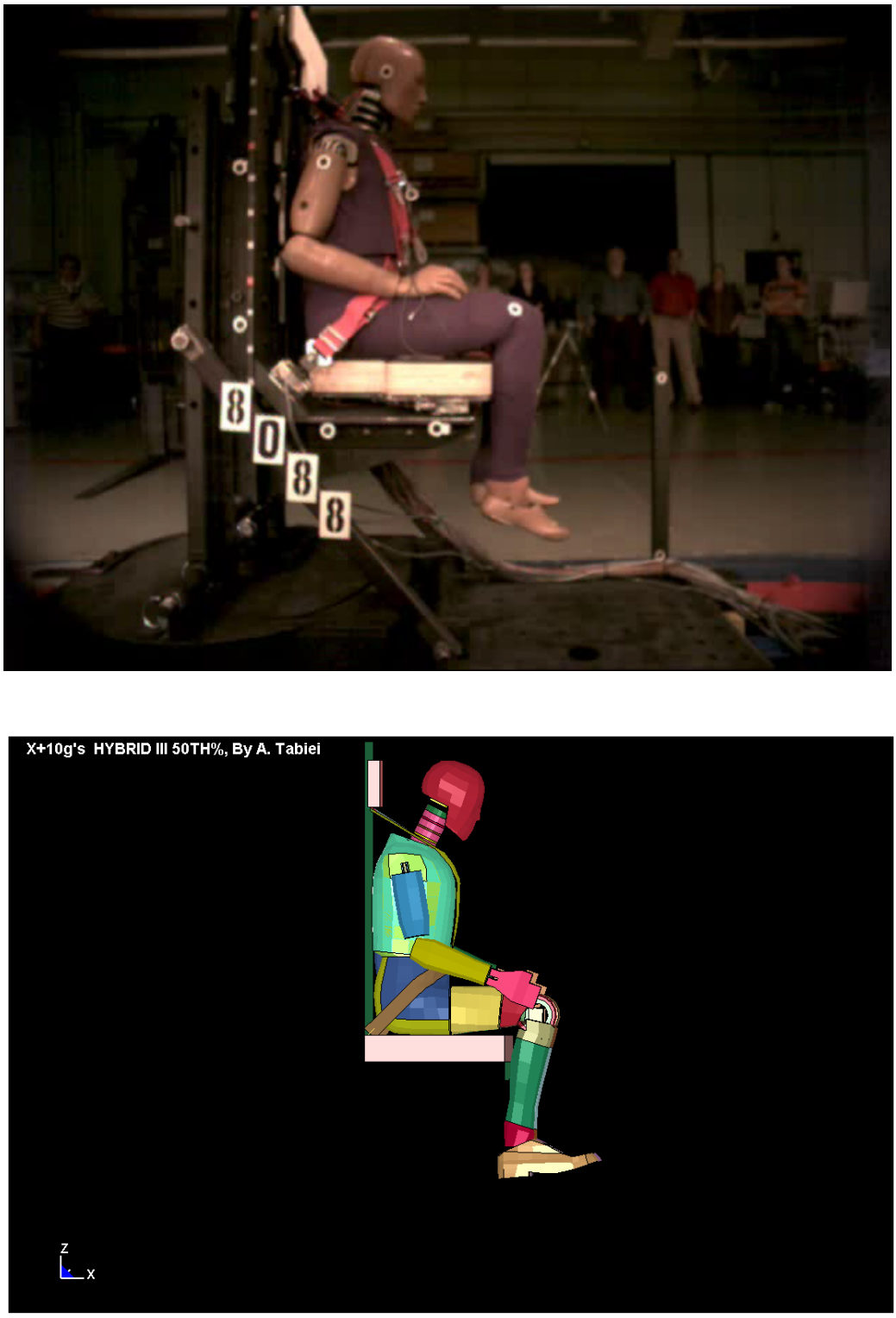

Figure 9. Physical dummy and the finite element dummy

Simulation Validation
+10 g's in the x-direction

The simulation of the belted dummy is carried out with LSDYNA version 971 on a PC using windows XP. The simulations required several hours to conduct a 300 millisecond simulation. The 300 millisecond is selected since there was no further significant response of the dummy to the applied pulse beyond this time. A sequence of photos are extracted from the movie of the test (WPAFB test #8088) using movie editing software. Unfortunately there was no timing synchronization between the tests and simulations available so the matching between the movies taken during the tests and the simulations can only be approximated. An attempt is carried out to extract photos of the simulation as close as possible to the timing on the movie. These sequences of events are shown in Figure 10.

The input pulse is shown in Figure 6 and consists of a near triangular pulse of 10 g's in the positive +x-direction. The positive x-direction is equivalent to a rear impact loading and is close to the loading direction that a crew member would be exposed to during a nominal CEV landing. In the test, this pulse is given to the entire seat assembly since the seat is firmly attached to a relatively rigid sled that is accelerated using a hydraulic jack that pushes the sled down a horizontal track. A wooden block is set between the seat pan and the physical dummy bottom in the test setup. A similar material is placed between the FE dummy bottom and the seat. The seat in the finite element model is assumed to be rigid and modeled using rigid shell elements. The seat is given an x-acceleration identical to the measured sled acceleration since it is assumed that the seat and sled move together as a single rigid unit. The finite element model did not include the seat/sled assembly and consequently the proper boundary conditions on the seat are in question since it is not completely clear how the actual sled accelerations transfer to the seat. To assess the effect of the boundary conditions two boundary conditions are considered in the simulation. The first boundary condition is the seat is assumed to be free to move freely in the y (sideways) and z (dummy spinal) directions. The second boundary condition is the seat is only allowed to move in the pulse direction, and the y and z-direction displacements are fully constrained. Both boundary conditions turned out to predict almost the same results.

Kinematics, force, and moment data from the simulation are collected at high frequency to include most of the responses. The corresponding data from the tests are collected at a frequency of one millisecond intervals. The head resultant acceleration from test and simulation is presented in Figure 11. The simulation data is filtered with a low by pass filter (ASE Filter) at 180 Hz and is also shown in Figure 11. The magnitude of the pulse from the simulation and test is very close to each other. However, one can observe that there are two peaks in the test results. This is not clearly understood. The test results indicate that there is a double impact event taking place between the physical dummy head and the pads on the seat behind the head. The double impact was also confirmed from the movies. This double impact is only possible if there was a slip between the head and the pads. In the finite element model the pads are modeled with crushable foam and only one impact event was predicted between the foam and the dummy head. Overall the magnitude of the head acceleration is reasonably close between the test results and the simulation.

The chest acceleration is extracted from the simulation and compared to the chest acceleration of the physical dummy in Figure 12. The simulation data is filtered with the same filter and cut off frequency of 180 Hz as the previous data. In here the experimental data is also in question. If the dummy is belted as reported and a tension is applied to the belts that securely hold the physical dummy to the seat, then the dummy chest should move with the seat and sled and the acceleration should match the input pulse. However, if there was a slip between the dummy and the seat belts, this would create an additional impact force on the dummy chest and cause a higher acceleration. The prediction from the finite element dummy at the chest location is similar to the input pulse as is anticipated since the FE dummy is modeled as constrained to move with the seat and sled.

The pelvis acceleration from the test and simulation is shown in Figure 13. In here a much better prediction is obtained and the pelvis acceleration of the finite element dummy matched the acceleration of the pelvis acceleration of the physical dummy very well.

Normally forces and moments are the hardest to match between FE simulation and test of dummies. Figure 14 depicts the neck y-moments from the test and the simulation. As discussed earlier, one can observe the timing issue and a phase difference between simulation and test results. In general the experimental data yielded a higher moment than the simulation. The head impacts the pads at about 70 milliseconds in the test of the physical dummy. One can see that the neck moment is positive up until the time when the head impacts the pad and the neck forces change over to negative. However, the head impacts the pads at a later time in the simulation. This explains the difference in the phase of the neck y-moment between the test and the simulation. If one shifts the simulation data in time, a better correlation is obtained.

The lumber forces which cause one of the most important injuries observed in fighter jet ejection seats and other similar events can be extracted from the finite element dummy. However, in general the dummy is not specifically designed to collect such data nor is it validated for predicting lumbar forces. The lumber column is modeled relatively primative in the Hybrid III dummy. For obtaining accurate lumber data a more elaborate dummy must be used, however for comparative purposes the Hybrid III model may be useful. The lumber z-force is shown in Figure 15. Lumber forces from the test and simulation are reasonably close. The lumber force in the x-direction is also collected and compared to the experimental data in Figure 16. However, the correlation is not as good as the z-forces. A similar trend is observed in the test and simulation.


X+10g's HYBRID III 50TH%, By A. Tabiei
Time = 30
Time = 50
Time = 69.999

Figure 10. sled test in the x-direction at 10 g's pulse

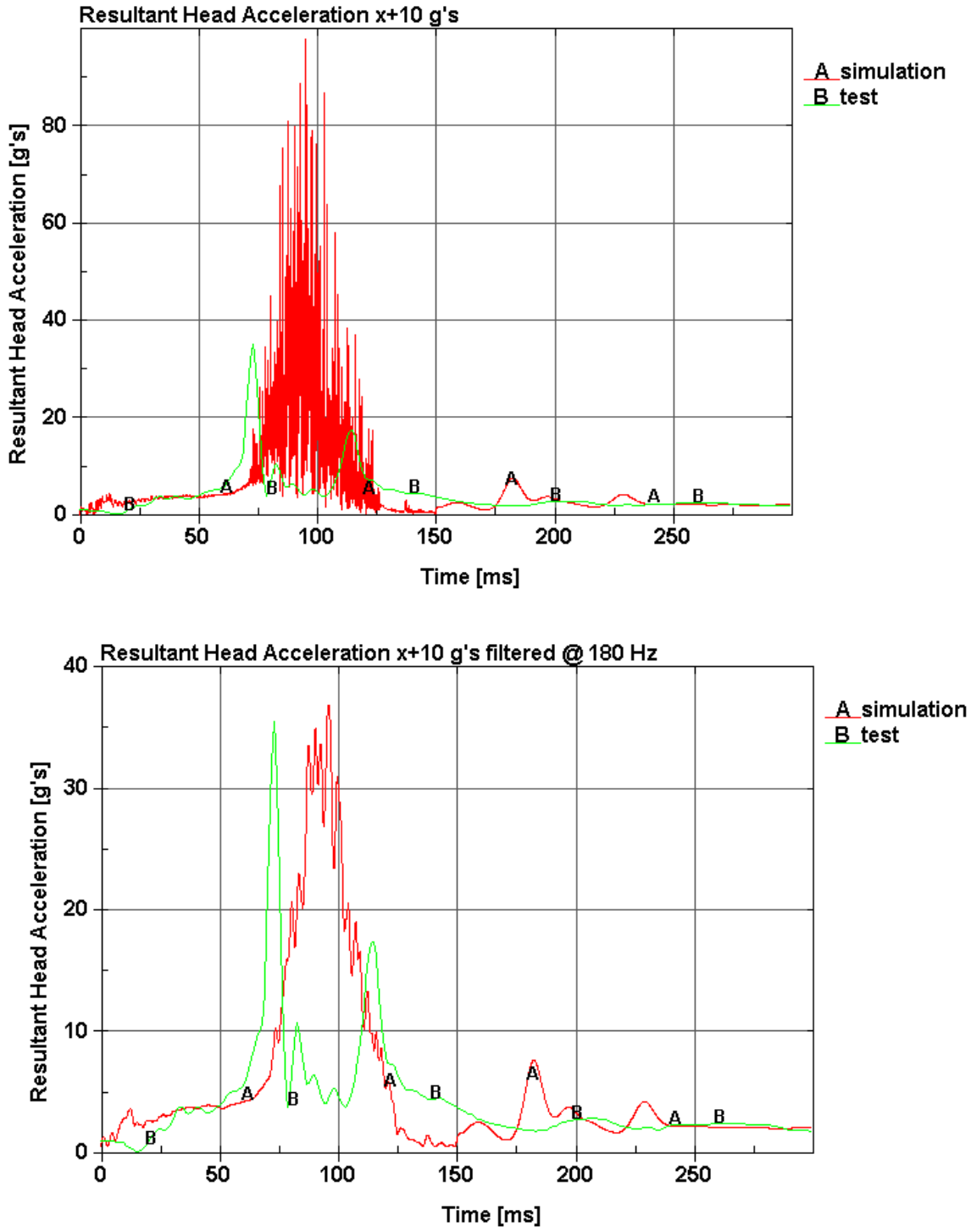

Figure 11. Hybrid III head acceleration from physical and FE dummy

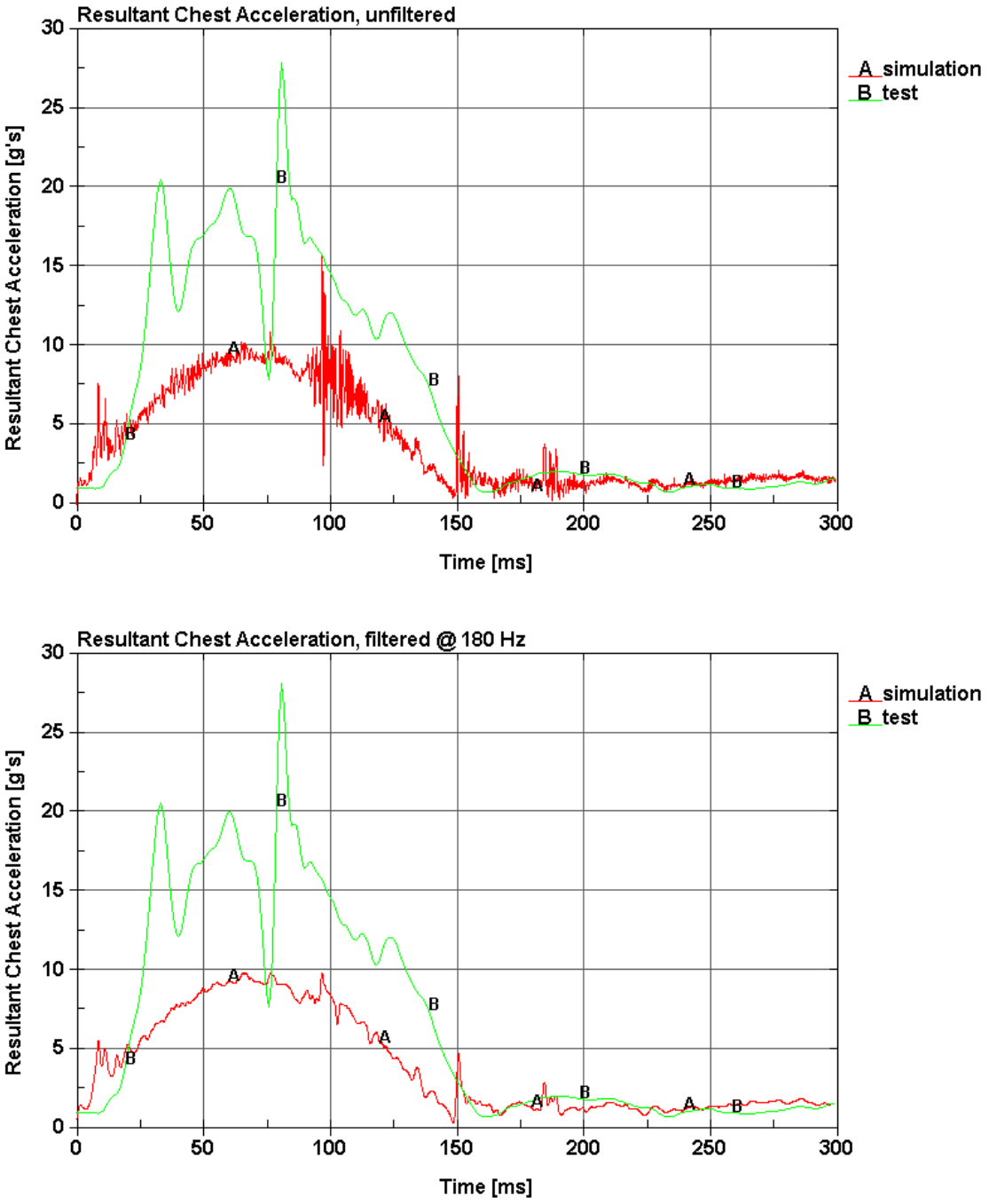

Figure 12. Hybrid III chest acceleration from physical and FE dummy

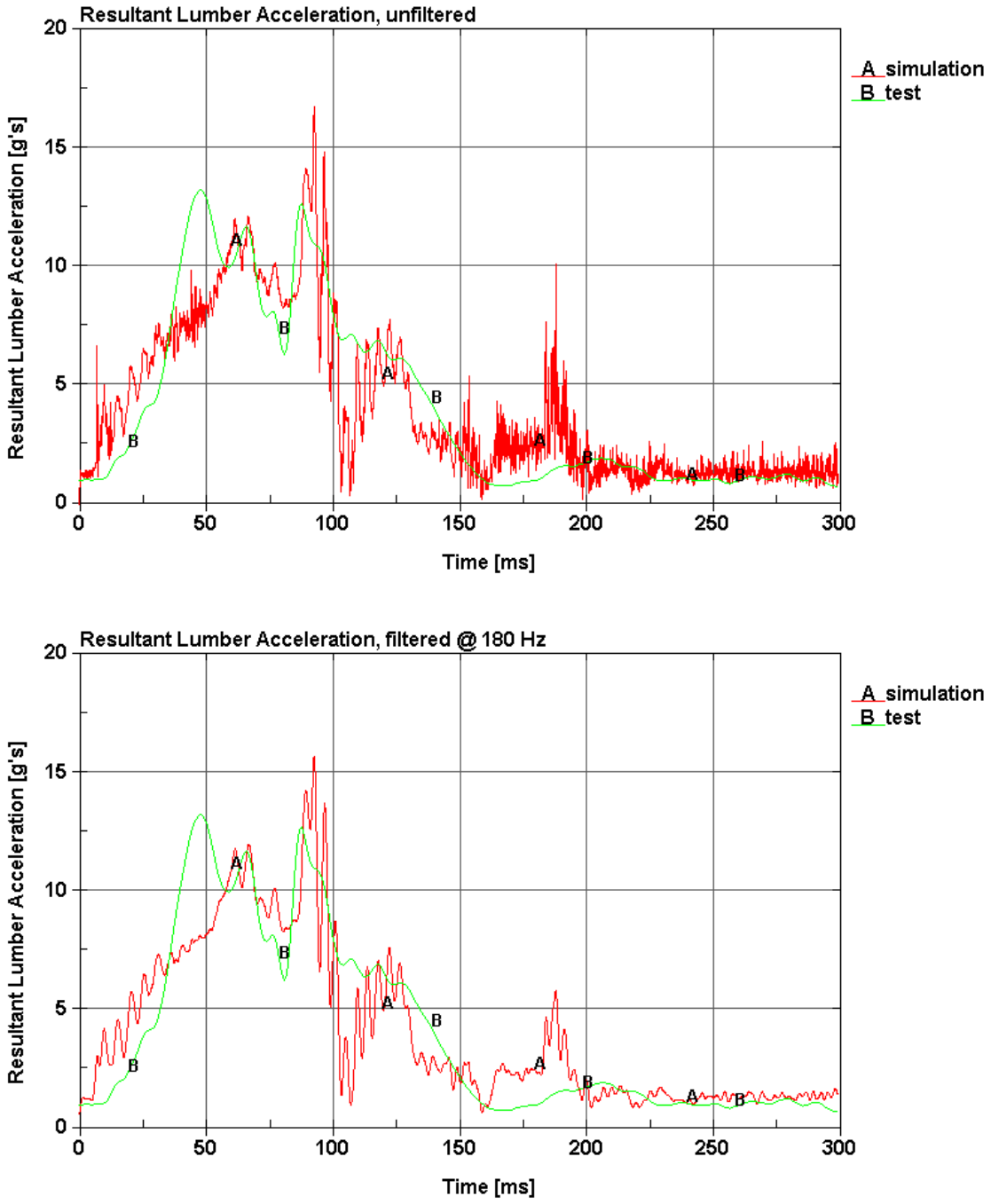

Figure 13. Hybrid III pelvis acceleration from physical and FE dummy

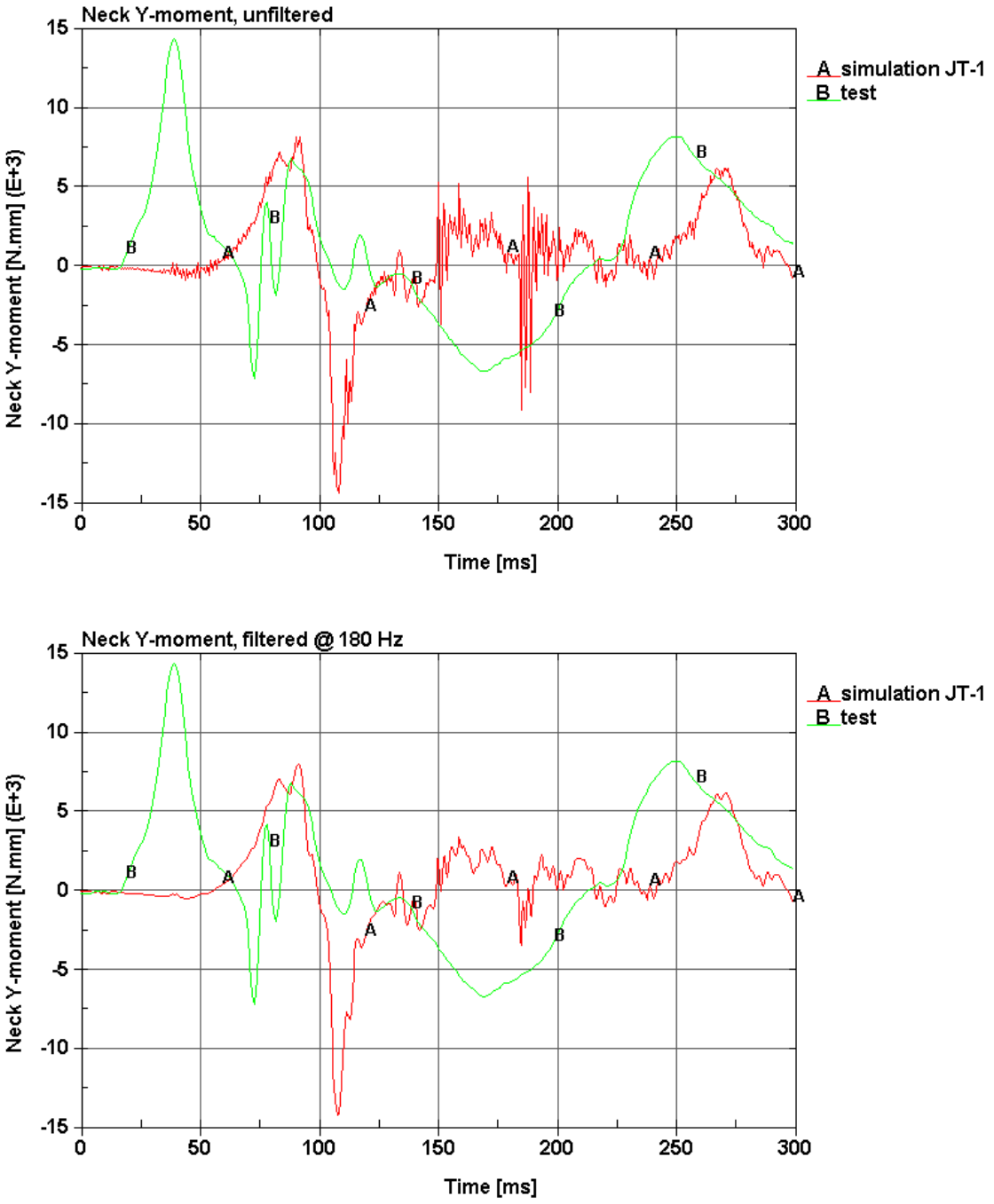

Figure 14. Hybrid III neck moment from physical and FE dummy

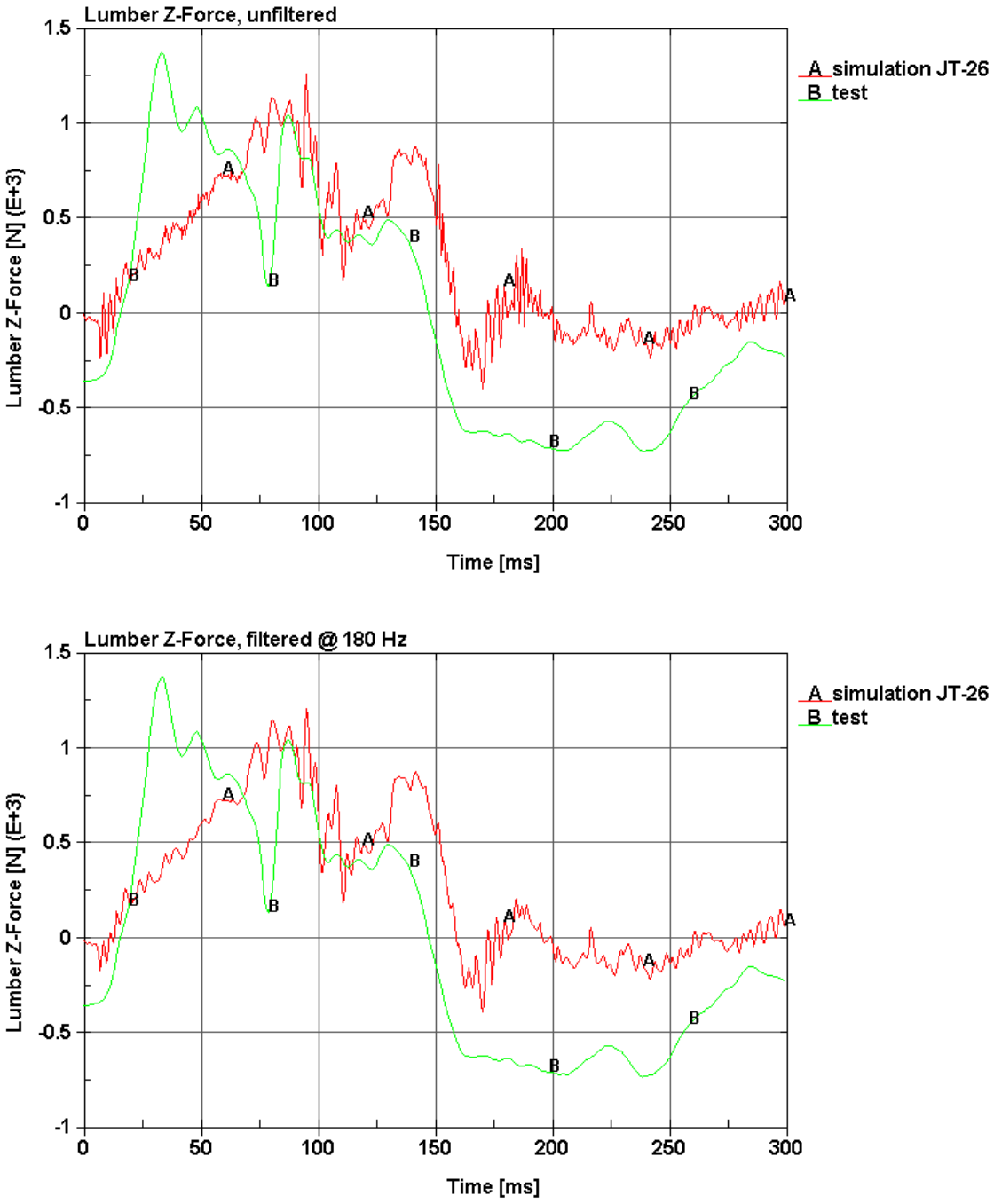

Figure 15. Hybrid III lumber z-force from physical and FE dummy

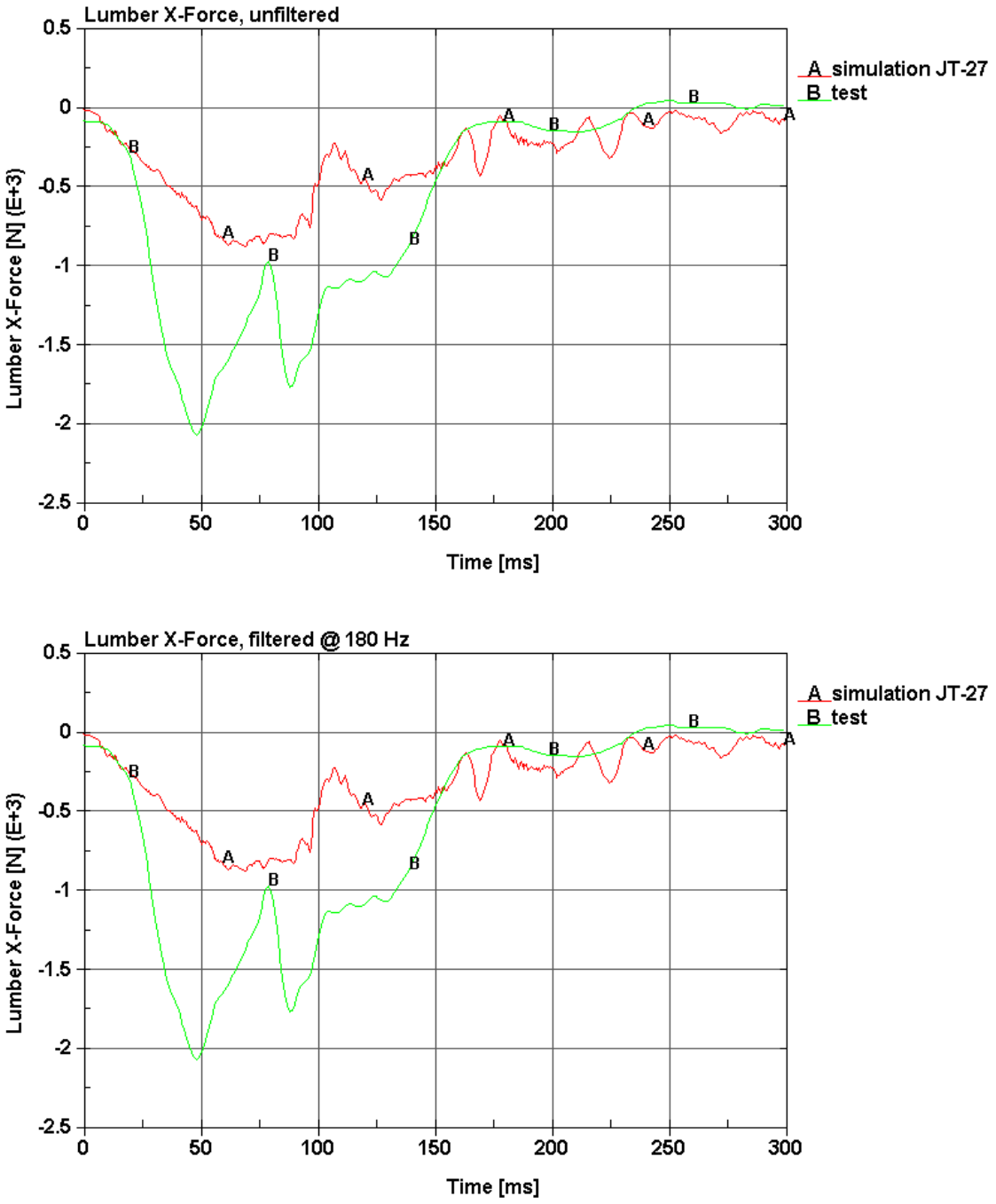

Figure 16. Hybrid III lumber x-force from physical and FE dummy

Injury Assessment

The experimental data obtained from the test can be used to determine the probability of injuries in such an impact event. The injury criteria listed in the previous sections are used to determine the injury values. Summary of the critical data with respect to some of the injury criteria listed in the previous section are listed in table 4.

Table 4. Injury assessment and critical injury values

Criterion name	Allowable	Predicted Test/Simulation	Pass/fail	Comments
HIC	700	129.8	pass	
CSI	700	28.7	pass	
Thorax g's	60 g's	27/10 g's	Pass	
Pelvis g's	130 g's	12/15 g's	Pass	
Lumber force	6672 N	1350/1250 N	Pass	
Neck force	6806 N	3950 N	Pass	
Neck moment flexion	310 N.m	14/8 N.m	Pass	
Neck moment extension	135 N.m	7/14.5 N.m	Pass	

Conclusion

An experimental effort is under taken by NASA to determine crew response during landing of the Orion vehicle for a variety or landing orientations and velocities and crew protection systems. This experimental effort consists of testing various Hybrid III physical dummies under different pulses in different directions. Finite element models of the test set up is developed with the Hybrid III 50% rigid/deformable dummy. These models are used for the validation. Kinematics data from the tests are compared to the predictions of the finite element models. In addition, forces and moments in the various physical dummy are collected and compared to the prediction of the corresponding parts in the finite element dummy model. In general good predictions by the finite element dummy is obtained. However, a better prediction is more possible if the test set up of the physical dummy better matched the positions of the finite element dummy before the testing is conducted.

Several injury criteria are presented in this paper. These injury criteria are developed and validated with respect to experimental observation. The criteria were collected over many years by various researchers. These injury criteria are used to determine the potential for injury value by comparing the allowable injury criteria values to the values produced from the tests and FE simulations.

References

[1] Tabiei A. and G. Nilakaltan, "Reduction of Crew Injury caused by Acceleration from Mine Blast/ IED", submitted to the Journal of Biomedical Engineering, 2007
[2] Fox, R.G., "OH-58 Energy Attenuating Crew Seat Feasibility Study," *U.S. Army Medical Research and Development Command, Fort Detrick, MD;Bell Helicopter-Textron Inc., Fort Worth, TX*, 1988,
[3] Simula Inc., "Aircraft crash survival design guide," *USAAVSCOM TR-89-D-22D*, 1989,
[4] Gowdy, V., "Development of a Crashworthy Seat for Commuter Aircraft," *CAMI, Federal Aviation Authority, Oklahoma*, September 1990,
[5] Laananen, D.H., "Crashworthiness Analysis of Commuter Aircraft Seats," *DOT/FAA/CT-TN91/28*, 1993,
[6] Haley, Joesph L., Jr., and Palmer, R.W., "Evaluation of a Retrofit OH-58 Pilot's Seat to Prevent Back Injury " 1994,
[7] Alem, N.M., and Strawn, G.D., "Evaluation of an energy-absorbing truck seat for increased protection from landmine blasts," *USAARL Report no. 96-06*, 1996,
[8] Night Vision and Electronic Sensors Directorate, "Tactical Wheeled Vehicles and Crew Survivability in Landmine Explosions," *AMSEL-NV-TR-207*, July 1998,
[9] Kellas, S., "Energy Absorbing Seat System for an Agricultural Aircraft," *NASA/CR-2002-212132*, December 2002,
[10] Keeman, D., "An engineering approach to crashworthiness of thin walled beams and joints in vehicle structures," *Thin Walled Structures*, Vol. 28, No. 3/4, 1997, pp. 309-320.
[11] Kai-Uwe Schmitt, Peter F. Niederer, Felix Walz: Trauma Biomechanics Springer Verlag, Berlin Heidelberg New York, 2004.
[12] Department of Army, "Occupant Crash Protection Handbook for Tactical Ground Vehicles," 2000,
[13] Horst, Marike van der, "Occupant Safety for Blast Mine Detonation under Vehicles," *10th MADYMO Users Conference*, 2003,
[14] Wayne State University, "Impact Testing Standards – BME 7170 Experimental Methods in Impact Biomechanics,"
[15] Tyrell, D., and Severson, K., "Crashworthiness Testing of Amtrak's Traditional Coach Set, Safety of High Speed Ground Transportation Systems," 1996,
[16] Gadd, C.W., "Use of a Weighted-Impulse Criterion for estimating Injury Hazard," *Proceedings, Tenth Stapp Car Crash Conference, SAE*, 1966,
[17] Armenia-Cope, R., Marcus, J.H., and Gowdy, R.V., "An Assessment of the Potential for Neck Injury Due to Padding of Aircraft Interior Walls for Head Impact Protection," August 1993,
[18] Kleinberger, M., Sun, E., and Saunders, J., "Effects of Head Restraint Position on Neck Injury in Rear Impact," February 1999,
[19] McHenry, B.G., "Head Injury Criteria and the ATB," 2004,
[20] R. Nirula, "Correlation of Head Injury to Vehicle Contact Points using Crash Injury Research and Engineering Network Data," *Accident Analysis and Prevention*, Vol. 35, 2003, pp. 201.
[21] Teng, T., Chang, F., and Peng, C., "The Study of Head and Neck Injury in Traffic Accidents," *Journal of Applied Sciences*, Vol. 4, No. 3, 2004, pp. 449-455.
[22] Welcher, J.B., and Szabo, T.J., "Relationships between Seat Properties and Human Subject Kinematics in Rear Impact Tests," *Accident Analysis and Prevention*, Vol. 33, 2001, pp. 289–304.
[23] Croft, A.C., Herring, P., and Freeman, M.D., "The Neck Injury Criterion: Future Considerations," *Accident Analysis and Prevention*, Vol. 34, 2002, pp. 247-255.
[24] Bostrom, O., Svennson, M., and Muser, M., "NIC Measurement Techniques and Result Interpretation," *NIC Meeting, Gothenburg*, 1998,
[25] Nusholtz, G.S., Domenico, L.D., and Shi, Y., "Studies of Neck Injury Criteria Based on Existing Biomechanical Test Data," *Accident Analysis and Prevention*, Vol. 35, 2003, pp. 777–786.
[26] LS-DYNA Keyword User's Manual, Version 971, Livermore Software Technology Corporation, May 2007.
[27] Brinkley, J. W., and Mosher, S. E., "Development of Acceleration Exposure Limits for Advanced Escape Systems," AGARD CP-472, April 1989